FLOW CONTROL OF DISTORTION NOISE IN TURBOFAN ENGINE INLETS.

V Kota Institute of Sound and Vibration Research, University of Southampton
M C M Wright Institute of Sound and Vibration Research, University of Southampton

1. INTRODUCTION

The current paper focuses its attention towards control of noise associated with the fan of an engine. One of the mechanisms of noise production from a fan is attributed to its interaction with flow non-uniformities which are present in the intake due to inherent non uniform geometry of the intake or the non-uniformity in the ingested flow itself. These flow disturbances can be random or periodic and they interact with the fan to produce unsteady blade forces which radiate in the form of tones as observed in a typical noise spectrum of the fan. This mechanism has been extensively studied and well documented in the open literature. Tyler and Sofrin [1] have explained the kinematics of the interaction mechanism and each tone is shown to be the result of a spinning acoustic disturbance whose spatial harmonic order is related to the harmonic order of the flow disturbance. In order for the spinning acoustic disturbance to propagate through the duct it should satisfy the duct acoustic cut-on condition and the make up of the tone is thus restricted to a finite number of modes that satisfy this condition. The amplitudes of these modes are related to the amplitudes of the harmonics of the periodic flow disturbance via the results for the blade unsteady forces from the theory of unsteady aerodynamics, the fluctuating forces being considered as dipole sources distributed on the fan blades and the radiated field being obtained through the well known Greens function technique as illustrated in Goldstein [2].

The technique adopted to control noise is through the use of flow distortions. The inherent flow non-uniformity generates the primary field and this can be controlled by producing a secondary field whose modal amplitudes and phases can be adjusted through variation in the intensity and extent of the flow disturbance introduced via the positioning of a circumferential array of cylindrical rods in the inlet of the fan. The current paper focuses on this technique which was investigated previously by a few researchers (Polacsek [3]). The approach followed here places emphasis on the theoretical model due to Goldstein [2] to utilize the relationship among the radiated field, the blade unsteady aerodynamic forces, and the flow distortions to obtain the acoustic response of the controllers.

2. METHOD

A tone comprises many modes, the number of these being limited to as many as those that satisfy the duct acoustic cut-on condition. Therefore the pressure in any harmonic, p_{sB}, at a defined location along the duct $x(r,\theta,z)$ is expressed as a sum of weighted modes. The equation for pressure at any upstream or downstream location along the duct is

$$p_{sB}(\mathbf{x}) = \sum_{m=-\infty}^{+\infty}\sum_{n=1}^{+\infty}\left(A_{mn}^{\pm} e^{-jK_{mn}^{+}z} + B_{mn}^{\pm} e^{-jK_{mn}^{-}z}\right)\Psi_{mn}(r,\theta), \quad (1)$$

where A_{mn} and B_{mn} represent the amplitudes of the forward propagating and backward propagating mode systems, the +/- superscripts on A_{mn} and B_{mn} refer to downstream/upstream

of the fan. $\Psi_{mn}(r,\theta) = \frac{J_m(\kappa_{mn} r)}{N_{mn}} e^{-jm\theta}$ represent the duct mode Fourier-Bessel shape functions with *m* and *n* being their circumferential and radial orders, and $N_{mn}^2 = \int_S J_m^2(\kappa_{mn} r)\, dS$ is the usual shape function normalisation factor. $k_{mn}^{z\pm} = \frac{\pm\sqrt{k_0^2 - \beta^2\kappa_{mn}^2} - Mk_0}{\beta^2}$ is the axial wave number related to the free space wave number k_0 and M, the flow mach number which accounts for the convective effect. The +/- superscripts on the axial wavenumber k^z_{mn} refer to those of either the backward or forward propagating mode. $A_{mn}^{\pm}$ and $B_{mn}^{\pm}$ are related through the reflection coefficients $R_{mn}^{\pm}$ as described by Morfey [4].

$$R_{mn}^{+} = \frac{B_{mn}^{+}}{A_{mn}^{+}} = e^{2j\eta_{mn}^{0+}}$$

$$\frac{1}{R_{mn}^{-}} = \frac{B_{mn}^{-}}{A_{mn}^{-}} = e^{2j\eta_{mn}^{0-}} \qquad (2)$$

$\eta_{mn}^{0\pm}$ is the complex reflection phase at the downstream/upstream duct ends. Restricting our attention to the upstream side of the fan in order to control the noise on the inlet side, pressure can be expressed in terms of the upstream backward propagating modal amplitude B_{mn}^{-}.

$$p_{sB}(\mathbf{x}) = \sum_{p=-\infty}^{+\infty}\sum_{n=1}^{+\infty} 2B_{mn}^{-} e^{j\left(-\eta_{mn}^{0-} + \frac{MsB\Omega}{c_0\beta^2}z\right)} \cos\left(\eta_{mn,sB}^{-}(z)\right) \Psi_{mn}(r,\theta) \qquad (3)$$

$\eta_{mn,sB}^{-}(z)$ is the complex reflection phase that varies along the axis and is given by

$$\eta_{mn}^{\pm}(z) = \eta_{mn}^{0\pm} + \frac{k_{mn}}{\beta^2} z \;,\; k_{mn} = \sqrt{k_0^2 - \beta^2\kappa_{mn}^2} \;. \qquad (4)$$

A mode of circumferential order *m* is excited by a flow disturbance of harmonic order *p*, the relationship between them being *m= sB-p*, where *B* is the number of blades and *s* is an integer. The modal amplitudes are obtained from a theoretical model (Goldstein [2]) that treats the blade fluctuating forces as dipoles sources for an infinite duct approximation. Pitelet [5] extended it to the case of a finite duct to take the end reflections into account. This was extended for a semi-infinite duct approximation to account for the case where there is an anechoic termination at the outlet. The expression for pressure that was obtained from such a treatment is given below. This expression relates the acoustic pressure field to the unsteady blade drag and thrust forces, $\hat{D}_{mn,p}$ and $\hat{T}_{mn,p}$. These unsteady forces are in turn related to the flow disturbance $w(r_s,\theta_s)$ through a Fourier-Bessel decomposition.

$$p_{sB}(x) = B\sum_{p=-\infty}^{\infty}\sum_{n=1}^{\infty} \frac{J_m(\kappa_{mn}r)e^{-jm\theta}}{N_{mn}^2 k_{mn,sB}} e^{-j\eta_{mn}^{0-}} (m\hat{D}_{mn,p} + \gamma_{mn,sB}^{-}\hat{T}_{mn,p}) e^{j\frac{MsB\Omega}{c_0\beta^2}z} \cos\left(\eta_{mn,sB}^{-}(z)\right)$$

$$= B\sum_{p=-\infty}^{\infty}\sum_{n=1}^{\infty} \frac{J_m(\kappa_{mn}r)e^{-jm\theta}}{N_{mn}^2 k_{mn,sB}} e^{-j\eta_{mn}^{0-}} (m\hat{D}_{mn,p} + \gamma_{mn,sB}^{-}\hat{T}_{mn,p})(1/2)\left(e^{j\left(\frac{MsB\Omega}{c_0\beta^2}z + \eta_{mn,sB}^{-}(z)\right)} + e^{j\left(\frac{MsB\Omega}{c_0\beta^2}z - \eta_{mn,sB}^{-}(z)\right)}\right) \qquad (5)$$

$$\gamma_{mn,sB}^{-} = -\frac{k_{mn,sB}}{\beta^2} - \frac{MsB\Omega}{c_0\beta^2} \qquad (6)$$

The factor in the amplitude for each mode, $(m\hat{D}_{mn,p} + \gamma_{mn,sB}^{-}\hat{T}_{mn,p})$, is called the coupling coefficient, $C_{mn,p}$.

$$\begin{cases} \hat{T}_{mn,p} \equiv -\frac{c}{2}\rho_0 U_t \sin\chi \ \sin\mu\, S_c(\sigma_p, M_t) W^T_{mn,p} \\ \hat{D}_{mn,p} \equiv -\frac{c}{2}\rho_0 U_t \cos\chi \ \sin\mu\, S_c(\sigma_p, M_t) W^D_{mn,p} \end{cases}, \quad \begin{cases} W^D_{mn,p} = \int_0^{a}\int_0^{2\pi} e^{-j\beta x} J_m(\kappa_{mn} r_s) w(r_s,\theta_s) \frac{1}{r_s} \mathrm{d}\theta_s \, \mathrm{d}r_s \\ W^T_{mn,p} = \int_0^{a}\int_0^{2\pi} e^{-j\beta x} J_m(\kappa_{mn} r_s) w(r_s,\theta_s) \, \mathrm{d}\theta_s \, \mathrm{d}r_s \end{cases}, \quad (7)$$

where S_c is the Sears function for a compressible flow and W^T and W^D are the Fourier-Bessel flow distortion harmonics.

The total acoustic field resulting from the presence of the controllers can be considered as a superposition of the primary field from the primary flow disturbance $w_{primary}(r,\theta)$ and the secondary field from the secondary flow disturbance $w_{secondary}(r,\theta)$. The coupling coefficient for the total or error field is as follows.

$$C_{error} = \left(C_{prim} + C_{secondary} \right) \quad (8)$$

The secondary flow disturbance is varied by adjusting the lengths and orientations of the control rods. To minimise the total field a cost function representing the sound power in a chosen number of harmonics of the error field is considered. The expression for power in a single harmonic for the case of fan was obtained by using an expression for the power of a propagating duct mode given by Morfey [4] which takes into account the reflections through modal admittances defined as $B_{sB,m,n} = \rho_0 c_0 p_{sB,m,n} / U_{sB,m,n}$, $p_{sB,m,n}$ being the pressure and $U_{sB,m,n}$ being the axial velocity. The expression for sound intensity mentioned in the above reference can be seen to be dependent on $B_{sB,m,n}$ which is a function of the complex reflection phase $\eta_{mn,sB}$. The complex reflection phase $\eta_{mn,sB}$ is resolved into real and imaginary parts $\xi_{mn,sB}$ and $\Phi_{mn,sB}$ respectively and the expression for power obtained by integrating the intensity over the duct cross section will be dependent only on the imaginary part $\Phi_{mn,sB}$ of the reflection phase.

$$P_{sB} = B^2 (1/\rho_0 c_0) \sum_{p=-\infty}^{\infty} \sum_{n=1}^{\infty} \frac{1}{N^2_{mn} k^2_{mn,sB}} \frac{\alpha_{mn,sB} \beta^4}{(1-\alpha^2_{mn,sB} M^2)^2} e^{2\phi^{0-}_{mn,sB}}$$

$$\times \left(\frac{e^{2\phi^{0-}_{mn,sB}}}{2} (1+\alpha_{mn,sB} M)^2 - \frac{e^{-2\phi^{0-}_{mn,sB}}}{2} (1-\alpha_{mn,sB} M)^2 \right) \left| (m\hat{D}_{mn,p} + \gamma^{-}_{mn,sB} \hat{T}_{mn,p}) \right|, \quad (9)$$

where $\alpha_{mn,sB} = k_{mn,sB} / k_0$.

The complex reflection phase $\eta_{mn,sB}$ is related to the reflection coefficient at the open end of the duct (inlet) R^{end-}_{mn} through the following expressions (Pitelet[5]).

$$\eta^{-}_{mn,sB}(z) = \frac{-\log R^{end-}_{mn,sB}}{2j} + \frac{k_{mn,sB}}{\beta^2}(z - L^{-}), \quad R^{end-}_{mn,sB} = R^{-}_{mn,sB}(L^{-}) = e^{-2j\left(\eta^{0-}_{mn,sB} + \frac{k_{mn,sB}}{\beta^2} L^{-}\right)}, \quad (10)$$

where L^{-} denotes the axial co-ordinate of the duct inlet.

The reflection coefficient at the duct end $R^{end-}_{mn,sB}$ is computed using the Weinstein U-function technique as outlined in Hocter [6] after neglecting inter-modal coupling. Excepting the term for the coupling coefficient which is dependent on the control vector, the rest of the terms in the above expression can be considered a constant specific to each mode and the resulting expression for power P_{sB} can be considered as

$$P_{sB} = \sum_{p=-\infty}^{\infty} \sum_{n=1}^{\infty} (modeconstant) \left| C_{mn,p} \right|^2 \tag{11}$$

The cost function J is now a summation of the powers in the number of harmonics chosen for optimisation.

$$J = \sum_{sB} P_{sB} = \sum_{sBmn,p} \sum \left(C_{error}^H C_{error} \right) x(modeconstant)$$

$$= \sum_{sBmn,p} \sum \left(C_{prim} + C_{secondary} \right)^H \left(C_{prim} + C_{secondary} \right) x(modeconstant) \tag{12}$$

In order to calculate the modal coupling coefficients of the controller rods a wake model for the wake profile $w_q(r,\theta)$ generated by each control rod q, as given in Polacsek [3], is assumed. This model assigns a normal distribution along the circumferential coordinate θ for the velocity distribution of a wake, w_q, generated by an infinitely long rod and was extended by Pitelet [5] to account for the edge effect of a finite rod of length l and diameter d located at (θ_o, z_0) along the duct.

$$w_q(r,\theta) = U \sqrt{\frac{d}{z_r}} e^{-\frac{\pi}{z_r \alpha}\left(\frac{r(\theta-\theta_o)}{0.8}\right)^2} e^{-\frac{\pi}{z_r \alpha}\left(\frac{z-l-r}{0.8}\right)^2} \tag{13}$$

The net coupling coefficient for the secondary field can be considered as a linear superposition of the coupling coefficients associated with each control rod.

$$C_{secondary} = \sum_{w} C_{mn,p,sB} \tag{14}$$

The cost function is now a function of the array of controller lengths and its orientation. If the orientation of the array is fixed, the cost function will then be a function of the control vector alone. This expression is minimised considering the derivative with respect to the control vector, $\boldsymbol{w}$ which is an array of lengths. Differentiating equation (12) with respect to $\boldsymbol{w}$ and realising that the primary coupling coefficient is a constant the following expression is obtained for the control vector derivative of the cost function.

$$\frac{\partial J}{\partial \mathbf{w}} = \sum_{sBmn,p} \sum 2\mathrm{Re}\left(\left(\frac{\partial C_{secondary}}{\partial \mathbf{w}} \right)^H C_{error} \right) x(modeconstant) \tag{15}$$

The control vector derivative of the cost function $\partial J / \partial \mathbf{w}$ is thus expressed in terms of the same with respect to the secondary field coupling coefficient $\partial C_{secondary} / \partial \mathbf{w}$. The control vector can be determined in either of the following ways.

(i) Linearised controller response.

$C_{secondary}$ is linearised with respect to $\boldsymbol{w}$ and the minimum of the cost function is obtained by setting the derivative of the cost function to zero.

$$\frac{\partial J}{\partial \mathbf{w}} = 0; \tag{16}$$

Denoting $\frac{\partial C_{secondary}}{\partial W} = G$, (17)

where G is the transfer function matrix for the linearised controller modal coupling coefficients,

$$G = \begin{bmatrix} g_{(mn,p)_1,sB_1} e^{-j\rho\beta_1} & \cdots & g_{(mn,p)_1,sB_1} e^{-j\rho\beta_v} \\ \cdots & \cdots & \\ g_{(mn,p)_u,sB_1} e^{-j\rho_u\beta_1} & \cdots & g_{(mn,p)_u,sB_1} e^{-j\rho_u\beta_v} \\ \cdots & \cdots & \\ g_{(mn,p)_{umax},sB_{vmax}} e^{-j\rho_{umax}\beta_1} & \cdots & g_{(mn,p)_{umax},sB_{vmax}} e^{-j\rho_{umax}\beta_v} \end{bmatrix}_{(max\ cutonmodes \times\ no.of\ controllers)} \quad (18)$$

The factor $g_{(m,n,p)}$ in each element of the matrix is the slope of the linearised coupling coefficient characteristic for each mode. The factor $e^{-j\rho\beta}$ is the factor for each rod to account for its phase shifting from the zero reference. Determination of the control vector then requires the inversion of the following matrix equation

$$\sum_{sBmn,p} \sum 2\mathrm{Re}\left(\left(G^H G\right)W\right)x(modeconstant) = -\sum_{sBmn,p} \sum 2\mathrm{Re}\left(G^H C_{prim}\right)x(modeconstant) \quad (19)$$

Though obtaining the control vector from the above matrix inversion seems to be simple in terms of computation, it can result in a non-feasible solution for the control vector wherein some or all of the controllers attain negative lengths.

(ii) Linearised controller response and constrained steepest descent algorithm.

A constrained steepest descent algorithm can be used to descend along the gradient of the cost function to iterate to a feasible optimal control vector. The constrained iteration of the control vector is performed as follows.

$$\mathbf{w}(k+1) = \mathbf{w}(k) - \mu \mathrm{Re}\left(\left(\frac{\partial C_{secondary}}{\partial \mathbf{w}}\right)^H C_{error}\right) + \beta_1\left(e^{\beta_2(r(k)-a)} - e^{\beta_2(r(k)-.3)}\right) \quad (20)$$

μ is the gradient step parameter, β_1 and β_2 are the parameters for the barrier function, and k is the iteration index.

The last term in the above expression is the penalty term introduced using the barrier function approach, as in Pitelet [5], the barrier being an exponential function that inhibits the control vector from straying into the non-feasible space, this being the satisfaction of the inequality $0 <= r <= a$, where a is the radius of the duct. The first of the exponential terms accounts for the barrier erected at the origin of the control vector space and the second one is for that erected at a control vector space location which corresponds to a value of $0.3m$ which is a little less than the radius a, which is $.315m$.

(iii) Non-linear approximation of the controller response and constrained steepest descent algorithm.

The error involved in the linearisation of the controller response poses a situation where the minimum residual power in the system obtained using the approximated response is higher than the power in the system without control. To avoid this, a non-linear approximation of the controller response is considered and the expression for the gradient of the cost function used in steepest descent algorithm is made to account for that. For the case of non-linear approximation of the response the transfer function $\frac{\partial C_{secondary}}{\partial W}$ is a matrix similar in size to G with each element being

$\left(\frac{\partial C_{(mn,p)_u,sB_v}}{\partial w} e^{-j p_v \beta_v}\right)$, where $\frac{\partial C_{(mn,p)_u,sB_v}}{\partial w}$ is the local gradient of the non-linear fit. As will be explained later in the discussion on results, the phase characteristic of the modal coupling coefficient is independent of length and the above gradient is that of the amplitude characteristic. The constrained iteration of the control vector is performed as mentioned in case (ii) above.

3. RESULTS

The methodology adopted here is to study the behaviour of the cost function *J*, by testing different combinations of (i) the primary disturbance, (ii) the number of controllers, i.e., the size of the control vector, (iii) the number of harmonics being optimised and (iv) also the approximation for the controller response. The cost function is then optimised using steepest descent algorithm which would output the optimum control vector w_{opt}. While equation (11) when evaluated using the approximated response for the optimal control vector gives the residual power for this case, the exact or the true value of this power has to be evaluated using the exact response resulting from the Fourier-Bessel decomposition for the same control vector, equation (7). This difference between the true and approximated estimates of the residual powers in the system gives an indication of the effectiveness of the approximation of the response.

For a given controller configuration, the optimum can also be seen to be dependent on the orientation or the phase of the controller array, and it makes sense to see how the control vector and the residual power vary with phase.

3.1 TEST CONDITIONS

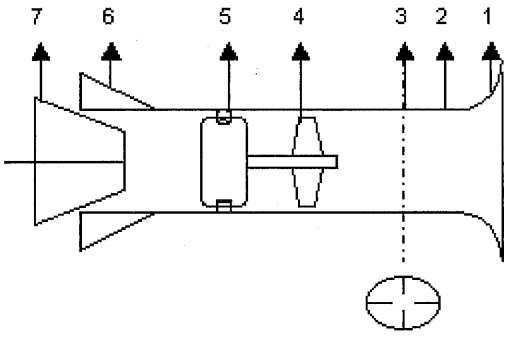

1. Nozzle 2. Duct 3. Controller 4. Fan 5. Motor 6. Silencer 7. Throttle

The results described here are for the simulation of optimisation that was conducted using the following parameters which correspond to those of the model fan rig that the system will finally be implemented on. The schematic of the fan rig with the wake generator is shown in figure1.
Ω, speed of the fan = 314 rad/s with the blade passing frequency = 50Hz.
B, no of the blades on the fan = 9.
D, tip diameter of the fan = 630 mm.
Control rod diameter = 20 mm.

Figure 1 Schematic of the fan rig with the wake generator

3.2 PRIMARY DISTURBANCE AND ITS MODAL AMPLITUDE DISTRIBUTION

A primary disturbance is assumed against which the optimisation behaviour of the controller array is tested. Figure 2 shows the crossbar defect – a velocity defect of magnitude 1m/s confined to a '+' shaped region. For the BPF of 50 Hz (*ka* = 0.2894)and its two harmonics considered, there can be a total of 30 cut-on acoustic modes. The modal amplitude distribution

for this defect is shown in figure 3. The cross bar induces acoustic modes of order *m* only for those flow distortion modes of order *p=4* and its multiples.

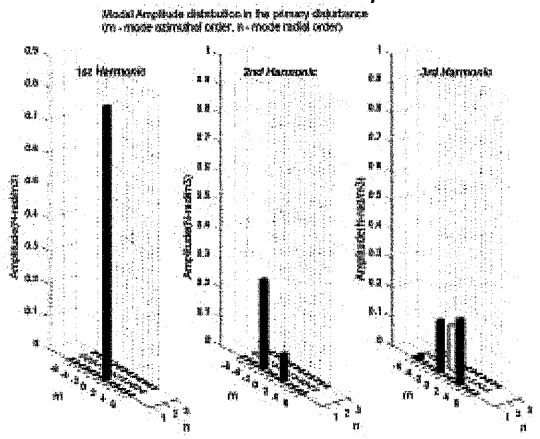

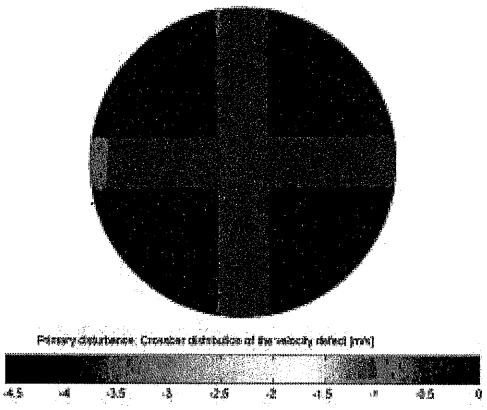

Figure 2 Primary disturbance (Crossbar type defect)

Figure 3 Modal Amplitude distribution in the primary disturbance

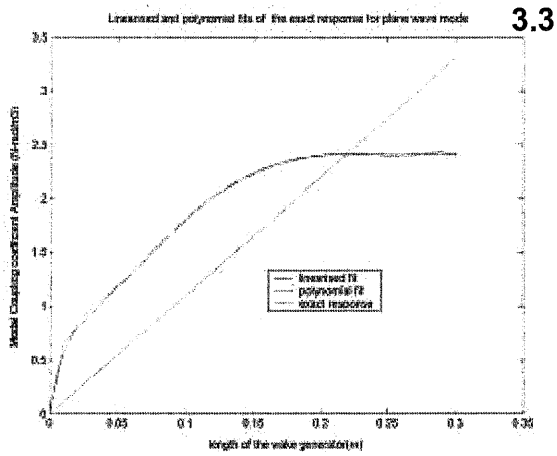

3.3 CONTROLLER RESPONSE (AMPLITUDE AND PHASE VARIATION WITH LENGTH OF RODS)

Figure 4 Amplitude response of the wake generator Figure 5 Cost function and controller its

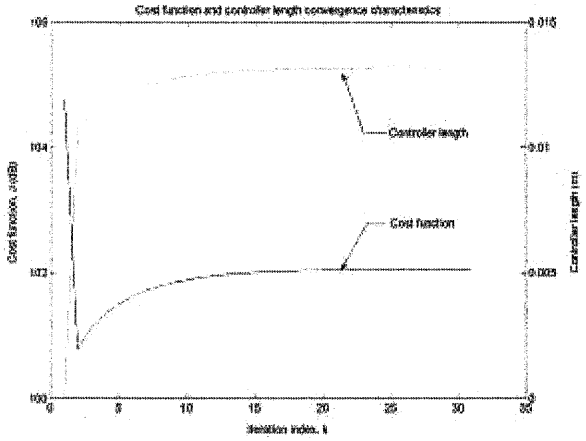

approximations length convergence characteristic

The controller is an array of equispaced control rods, each of diameter 20mm. The acoustic response, i.e, modal coupling coefficients, of the interacting flow wake generated by a single rod located at a reference zero azimuth location in the duct cross section is estimated numerically by substituting the expression for the wake profile in the Fourier-Bessel decomposition expression, equation (7). The length of the rod is varied as the rod is made to progressively protrude radially into the duct, and the resulting variation of the coupling coefficient is estimated in terms of its amplitude and phase. The amplitude variation alone is shown in figure 4 for the case of plane wave mode $m=0$. The phase variation, which is not shown here, is a constant with respect to the control rod length as the Fourier-Bessel decomposition being performed is that on a wake profile symmetric around the zero azimuthal reference. The variation in the amplitude is a rising characteristic within a certain interval of the controller length after which it tends to flatten out through a sharp curvature. This variation in the amplitude can be attributed to the Fourier and Bessel terms in the decomposition of the wake profile. The variation in the amplitude characteristics of the other modes is similar to what is shown for the plane wave mode and they are not shown here. As the amplitude variation seems to exhibit a strong non-linear behaviour and the exact response cannot be used in the optimisation of the cost function, it remains to be seen as to what the effect of its approximation, either linear or non-linear would be. Included in figure 4 are also the linear and an 8^{th} degree polynomial approximation of the exact response of the coupling coefficient amplitude for the plane wave mode. The effect of these approximations is explained in the next section.

3.4 OPTIMISATION

3.4.1 CONVERGENCE CHARACTERISTICS

For a fixed controller array orientation and an initial condition of zero for the control vector steepest descent algorithm is used. For the optimisation of two harmonics with an equispaced 4-rod controller array, whose phase/orientation is 22^0, the convergence characteristics are shown in figure 5 for the cost function (total power) and one of the controller lengths, both plotted against the iteration index k of the steepest descent algorithm. The convergence to optimum can be seen to be attained within 20 iterations.

3.4.2 RESIDUAL POWER, OPTIMAL CONTROL VECTOR LENGTH VARIATION WITH PHASE OF CONTROLLER ARRAY

The phase of the array is varied through an angle and for each orientation of the array the converged cost function/residual power and the optimal array lengths are determined. The optimisation was carried out initially for (a) a cost function based on linearised response without constraint, (b) and that with constraint; and finally for (c) a cost function based on the 8th degree polynomial approximated response with constraint. While (a) and (b) illustrate the effect of linearisation, (c) shows the same for a non-linear approximation of the response. In the plots that follow, the minimal residual power is determined for (a), (b) and (c) using the approximated response of the controller through equation (11). For the optimal control vectors obtained in cases (b) and (c) the exact residual power in the system is also evaluated by substituting the wake distribution generated by the controller configuration in the expression for Fourier-Bessel decomposition. Both the exact and approximated residual powers are compared with primary power that is present in the system without control.

Figure 6 offers such a comparison for the 4-rod, 2-harmonic optimisation among the residual powers obtained in cases (a) and (b), the exact residual power in (b) and the primary power. Figure 7 shows the optimal controller lengths for the constrained and unconstrained cases. The powers are shown in the plot against the phase of the array, which is varied through 90^0 as the 4-rod controller configuration is azimuthally symmetric. The variation in the residual powers follows a sinusoidal pattern. Though the residual power for the unconstrained case shows that it is less than the primary power over several extents of the phase of the array, at exactly alternate extents of the phase the resulting minima can be seen to be accompanied by the outcome of the controller lengths being negative as seen in figure 7 for the unconstrained case. Although this condition is avoided using the barrier function technique for constrainment and the residual power obtained in this case exhibits a minimum only when the controller lengths are positive, the exact residual power seems to be higher than both the primary and the approximated residual power. The error between the exact and approximated residual powers is attributed to the error involved in approximation of the controller response through linearisation.

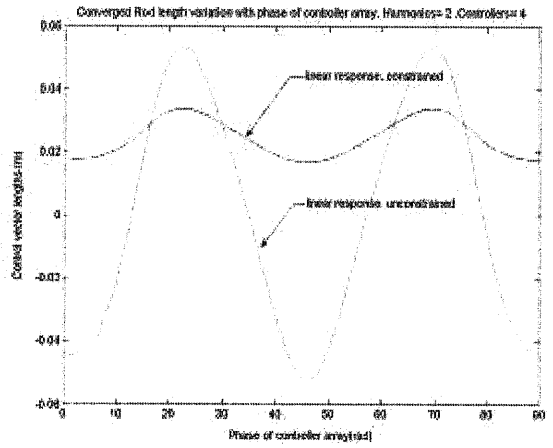

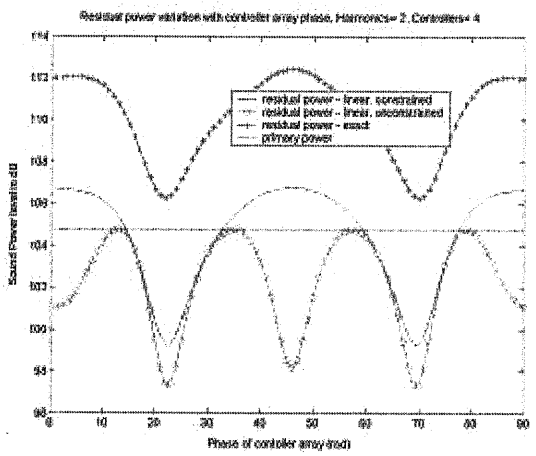

Figure 6 Residual power variation with controller

Figure 7 Controller length variation with array phase.

controller array phase.

Figure 8 offers a similar comparison among the approximate residual power obtained in (c), the exact residual power in (c) and the primary power. This plot shows the residual powers varying in the same pattern described above. The error between exact and approximated residual powers can be seen to be less in the case of a non-linear approximation than that illustrated for the linearised case above. The exact and approximate responses suggest that a maximum reduction in power of the order of *2 dB* can be obtained using the 4-rod equispaced controller with the each rod being *13mm* in length and the phase of the array being either 22^0 or 70^0. This reduction is specific to the primary disturbance considered and will vary depending on the primary disturbance chosen. The feasible phase locations mentioned above are nearly the same locations where the controller generated secondary acoustic mode of azimuthal order *m=1 (p=8* flow mode) is out of phase with respect to the corresponding primary disturbance mode. This is the dominant mode induced by the crossbar primary disturbance in the first harmonic and for the case of unconstrained optimisation the residual power approaches a minimum which is less than the primary power at 16 locations of the controller array phase. This can be considered as a *p=8* cycle sine lobe pattern which has 8 azimuthal locations where the mode is out of phase with respect to the other 8 locations. The residual power variation plot showed just 2 of those locations in the 90^0 degree azimuthal extent and the rest of those out-of-phase locations can be thought to be spaced equally apart at exactly the same locations as in the sine lobe pattern discussed above. The approximate residual power variation does not closely follow the exact estimate in those phase extents where control is not feasible and the controller length must constrain within an interval [0, .01] m of rod length which is where the polynomial approximation also deviates substantially from the exact response.

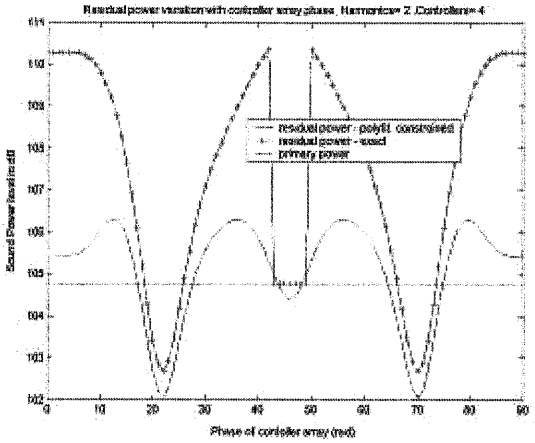

Figure 8 Residual power variation with controller array phase for polynomial fit of response

Simulation is being carried out for other cases of primary disturbances and an attempt is also being made to include the phase of the controller array also as one of the control or optimisation variables. Implementation of the system is being carried out on a model fan rig with a motion control system consisting of equispaced stepper motor actuated cylindrical rods. The error field will be modally decomposed using microphone sensor rings located in the inlet duct of the fan, and the optimum control vector will be iteratively approached using the same algorithm that was used for simulation.

4. CONCLUSIONS:

The simulation of active control of fan tones was performed using a choice of primary disturbance, a given number of controllers, and a given number of harmonics being optimised. For the particular case of a primary disturbance, namely the crossbar pattern, the optimisation performed using a constrained steepest descent algorithm revealed that
(i) A non-linear approximation rather than linearisation of the response for the controller gives a better indication of whether the residual power in the system is less than the primary power after control.
(ii) The residual power thus obtained has an order of variation with respect to the controller phase that is synonymous with the p order of the dominant mode in the primary disturbance

5. ACKNOWLEDGEMENTS:

This work was supported by EPSRC grant GR/M85296/01.

6. NOTATION:

Symbols

a duct radius
A_{mn} amplitude of forward propagating mode
B, B_{mn} number of blades, amplitude of backward propagating mode, modal admittance
c, c_0 blade chord, sound speed in air
$C_{mn,p}$ Mode specific coupling coefficient
d diameter of the control rod
$\hat{D}_{mn,p}$ Drag component
G Transfer function matrix for linear approximation of response
H Hermitian form
J_m, J Bessel function, optimisation cost function
$k, k_0, k_{mn,sB}, k_{mn}^{z\pm}$ iteration index, acoustic wave number (ω / c_o), mode characteristic wave number, axial wave number
l, L length of the control rod, length of inlet duct
m azimuthal mode number
M, M_r axial component of flow Mach number, blade relative flow Mach number
N_{mn} normalization factor for duct mode shape function
p pressure; azimuthal mode number of aerodynamic disturbance
P_{sB} Power in a harmonic sB
R Reflection coefficient
n radial mode number
x position vector
z axial coordinate
r, r_s radial coordinate, radial coordinate of the location of source
s integral multiple
$\hat{T}_{mn,p}$ Thrust component
U_r, U Relative velocity, mean flow velocity
$w(r,\theta), \boldsymbol{w}$ flow disturbance distribution, control vector distribution
W^T, W^D Intensity of flow Fourier-Bessel harmonic
S, S_c Duct cross sectional surface, Sears function
β, β_1, β_2 Mach number parameter, parameters of barrier function
$\xi_{mn,sB}$ Real part of reflection coefficient
$\phi_{mn,sB}$ Imaginary part of reflection coefficient phase
$\gamma_{mn,sB}$ parameter
σ_p Sears function parameter
κ_{mn} factor to fit cylindrical shape function across the cross section of duct(zeros of first derivative of cylindrical Bessel functions)
$\eta_{mn,sB}$ mode specific phase of reflection coefficient
ρ_0 density of air
μ blade angle of attack, steepest gradient step length
χ blade stagger angle
Ψ_{mn} duct mode shape function
Ω angular frequency of rotational fan
θ, θ_s azimuthal coordinate, azimuthal coordinate of the location of the source

Subscripts

sB	Blade mutiple(usually of the harmonic)
m,n	mode configuration(azimuthal order, radial order)
error	Error field
primary	primary field
secondary	secondary field

Superscripts

$+/-$	downstream/upstream locations along the duct
0	Reference location in the duct (at the fan)
$*$	Complex conjugate

7. REFERENCES:

[1] J.M. Tyler and T.G. Sofrin, "Axial flow compressor noise studies", 1961, SAE aeronautic meeting, 345D.
[2] M.E. Goldstein , "Aeroacoustics", 1976, McGraw-Hill, Inc.
[3] Polacsek C., "Reduction of fan rotor-stator interacting modes using a novel design: an experimental study", 6th International Congress on Sound and Vibration, 5-8 July 1999, Copenhagen, Denmark.
[4] Morfey C.L., "Sound transmission and generation in ducts with flow", JSV (1971) **14** (1), 37-55.
[5] C. Pitelet, "Flow control for fan noise reduction", 2000, M.Sc. Thesis, Institute of Sound and Vibration Research.
[6] Hocter S.T., "Sound reflection into a cylindrical duct", Proc. of The Royal Society, London A (2000) **456**, 2707-2716.